5

DAILY AND SEASONAL ENCODING OF RHYTHMS IN BROWN ADIPOSE TISSUE ACTIVITY

Sander Kooijman*
Rosa van den Berg*
Ashna Ramkisoensing
Laura Sardon Puig
Claudia P. Coomans
Johanna H. Meijer
Nienke R. Biermasz†
Patrick C.N. Rensen†

*Authors contributed equally
†Authors share last authorship

In preparation

Abstract

Brown adipose tissue (BAT) contributes importantly to non-shivering thermogenesis by its ability to combust large amount of triglycerides (TG) into heat. Interestingly, BAT is not only connected through the sympathetic nervous system to the hypothalamic temperature center but also to the suprachiasmatic nucleus (SCN). The SCN drives circadian (i.e. 24h) rhythms and activity of the SCN is known to adapt to seasonal changes in photoperiod. However, the effects of SCN on circadian and seasonal rhythms of BAT activity are largely unknown. Therefore, the aim of this study was to identify circadian and seasonal rhythms in BAT activity. Hereto, C57Bl/6J male mice were subjected to a short photoperiod of 8h (reflecting winter), a regular photoperiod of 12h or a long photoperiod of 16h (reflecting summer) per day. After 5 weeks, we assessed the uptake of TG-derived fatty acids from the circulation by BAT and other metabolically active tissues along the day. Under regular photoperiod, the various BAT depots showed a strong circadian rhythm in the uptake of fatty acids with a peak at ZT (Zeitgeber time) 12, just before the onset of the dark period. Strikingly, exposure to short photoperiod advanced the peak to ZT8 and increased the average diurnal fatty acid uptake, compared to long photoperiod that both delayed the peak and reduced the average fatty acid uptake. Similarly, short photoperiod resulted in an advanced onset of sympathetic outflow and expression of key thermogenic genes. Interestingly, this strong diurnal rhythm in fatty acid uptake as well as the adaptation to long and short photoperiod did not occur in other metabolically active tissues, including white adipose tissue, muscle and heart. In dyslipidemic APOE*3-Leiden. CETP mice exposed to a 10h photoperiod, at ZT10 compared to ZT0, the plasma half-life of TG-derived fatty acids was 1.6-fold lower, while the uptake of fatty acids by BAT was 4-fold higher, and plasma TG levels were 2.4-fold lower. In conclusion, our findings show that BAT activity is strongly regulated by the biological clock, incorporating both seasonal (i.e. photoperiod) and circadian information, which may contribute to circadian rhythms in plasma lipid levels.

Introduction

While the main function of white adipose tissue (WAT) is the storage of surplus energy in the form of triglycerides (TG), brown adipose tissue (BAT) combusts large amounts of TG into heat, a process called non-shivering thermogenesis. The thermogenic capacity of BAT arises from uncoupled respiration through expression of uncoupling protein-1 (UCP-1) and is initiated by sympathetic nervous system activity upon exposure to cold. Interestingly, retrograde tracing has not only identified direct neuronal connections between the hypothalamic temperature center and BAT, but also direct connections between the suprachiasmatic nucleus (SCN) and BAT (1).

The SCN is the central biological clock, responsible for the regulation of daily (*i.e.* circadian) rhythms in *e.g.* sleep-wake activity, endocrine function and body temperature. Administration of the excitatory neurotransmitter glutamate directly into the SCN increases BAT temperature (2), suggesting that an increased neuronal activity in the SCN may directly increase BAT activity. Accordingly, the expression of several nuclear receptors as well as the key thermogenic protein UCP-1 follows a circadian rhythm in BAT (3), and mice have a lower cold tolerance in the light phase than during the dark phase (4). Collectively, these data indicate functional differences in BAT reactivity throughout the circadian cycle.

The SCN also functions as a seasonal clock through adaptation to seasonal changes in daily photoperiod (5). This sophisticated timing system evolved in order to anticipate cyclic challenges, such as changes in food availability and temperature. Interestingly, detectability of human BAT by [^{18}F]fluorodeoxyglucose (FDG) PET-CT scans at room temperature follows a circannual cycle, with low detectability of BAT in summer as compared to winter (6). Although differences in outside temperature over the year would be a likely explanation for this phenomenon, the detectability of BAT showed a stronger correlation with photoperiod than with outside temperature (6).

We recently demonstrated in mice that prolonged daily light exposure (*i.e.* 16h and 24h of light per day compared to 12h of light per day) decreases sympathetic outflow towards BAT and reduces BAT activity (7). Since the effects of the SCN on more refined rhythms in BAT function are largely unknown, the aim of this study was to identify daily and seasonal rhythms in BAT activity. Thereto, we examined the daily rhythms in BAT with respect to changes in histology, gene expression and fatty acid uptake, and identified the effects of short photoperiod (reflecting winter) and long photoperiod (reflecting summer) on rhythmicity of BAT activity.

Materials & Methods

Animal studies

All animal experiments were approved by the institutional ethics committee on animal care and experimentation at Leiden University Medical Centre (LUMC), Leiden, The Netherlands. 12 week old male C57Bl/6J mice (Charles River) were single housed in clear plastic cages within light-tight cabinets at constant room temperature of 22°C. The cages were illuminated with white fluorescent light with an intensity of approximately 85 μW/cm^2. Before start of the experiment, mice were kept on a regular 12h:12h light-dark cycle. Mice were matched on body weight. Light intervention consisted of subjecting mice to a photoperiod of either 8, 12 or 16h of light per day (*i.e.* 24h) for the duration of five weeks (n=24 per group). Mice had *ad libitum* access to standard laboratory chow (Special Diets Services, UK) and water throughout the experiment. After being exposed to a specific photoperiod for five weeks, a TG-derived fatty acid uptake experiment (see below) was performed at time points ZT (Zeitgeber Time, time after lights on) 0, 4, 6, 8, 12 and 18 (n=4 per specific photoperiod per time point). At the end of this experiment, mice were sacrificed via cervical dislocation and organs were collected for further gene expression and histological analysis (see below).

Homozygous human cholesteryl ester transfer protein (*CETP*) transgenic mice were crossbred with hemizygous *APOE*3-Leiden* mice at our Institutional Animal Facility to obtain female *APOE*3-Leiden.CETP* mice on a C57Bl/6J background (8). Before start of the experiment, mice were kept on a regular 12h:12h light-dark cycle and matched on body weight and plasma TG. Mice were single housed on a photoperiod of 10h per day and had *ad libitum* access to Western-type diet (containing 16% fat and 0.1% cholesterol; AB diet, Woerden, the Netherlands) and water throughout the experiment. After 4 weeks, a TG-derived fatty acid uptake experiment (see below) was performed both at the onset of light (ZT0) and the onset of darkness (ZT10).

TG-derived fatty acid uptake

After 5 weeks of exposure to a specific photoperiod, the uptake of TG-derived fatty acids was assessed. Glycerol tri[^{3}H]oleate-labeled lipoprotein-like emulsion particles (80 nm) were prepared as previously described (9). Mice were fasted for 4h and intravenously injected with the radiolabeled emulsion particles (1.0 mg TG in 200 μL PBS) via the tail vein. Two mice could not be injected (12h ZT6 and ZT18). Blood was collected after 2, 5, 10 and 15 min to determine plasma decay of the radiolabel. After 15 minutes, mice were euthanized by cervical dislocation and perfused with ice-cold PBS for 5 min. Organs were harvested, weighed, and the uptake of ^{3}H-derived activity was determined.

Histology

Formalin-fixed paraffin-embedded iBAT sections were cut (5 µm). To determine sympathetic activation of iBAT a TH staining was performed. Sections were rehydrated and incubated 15 min with 10 mM citrate buffer (pH 6.0) at 120°C for antigen retrieval. Sections were blocked with 5% BSA/PBS followed by overnight incubation with anti-TH antibody (1:2000, AB-112, Abcam) at 4°C. Next, sections were incubated with a secondary antibody (anti-rabbit antibody, DAKO enVision), stained with Nova Red and counterstained with Mayer's haematoxylin. Percentage of area positive for TH staining was quantified using Image J software.

Gene expression analysis

A part of iBAT was snap frozen and stored at -80°C for gene expression analysis. Total RNA was isolated using TriPure (Roche) according to the manufacturer's instructions. 1 µg of total RNA was reverse-transcribed using M-MLV reverse transcriptase (Promega, Madison, WI, USA). Real-time PCR was carried out on a CFX96 PCR machine (Bio-Rad) using IQ SYBR-Green Supermix (Bio-Rad). Melt curve analysis was included to assure a single PCR product was formed. Expression levels were normalized to *36B4* and *Hprt* housekeeping gene expression. Data were plotted as relative expression to expression in 12h light group at ZT0. Primer sequences are shown in Table S1.

Plasma TG concentration

After 5 weeks, blood was collected from the tail vein of 4h fasted mice. Plasma was assayed for TG using a commercially available enzymatic kit (Roche, Mannheim, Germany).

Statistical analysis

Data are presented as means ± SEM. Contribution of Zeitgeber time and photoperiod to TG-derived FA uptake was analysed by two-way ANOVA. Differences between groups were determined by T-tests (for two groups) or using one-way ANOVA (more than two groups). Graph Pad Prism v6.0 was used for all calculations. Associations of variables with day length exposure as independent variable were assessed by linear regression analysis. Differences at p values < 0.05 were considered statistically significant.

Results

TG-derived fatty acid uptake shows circadian rhythm in metabolic organs, most pronounced in BAT

To study the daily and seasonal rhythms in BAT activity, C57Bl/6J male mice were exposed to a photoperiod of 8h (short), 12h (regular) or 16h (long) per day. After 5 weeks, we determined the ability of BAT and other metabolic organs to take up TG-derived fatty acids at 6 different Zeitgeber time (ZT) points (0, 4, 6, 8, 12 and 18).

First, we identified daily rhythms in the uptake of [^{3}H]oleate from glycerol tri[^{3}H]oleate-labeled lipoprotein-like emulsion particles under the standard laboratory photoperiod of 12h. Zeitgeber time determined the uptake of [^{3}H]oleate in liver, subcutaneous WAT (sWAT), gonadal WAT (gWAT), heart, muscle, interscapular BAT (iBAT), subscapular BAT (sBAT) and perivascular adipose tissue (PVAT) (all p-values for ZT, $p_{ZT} \leq 0.01$; **Figure 1A-H**). The peak in uptake of ^{3}H-activity was found at ZT18 for liver (**Figure 1A**), sWAT (**Figure 1B**) and gWAT (**Figure 1C**), corresponding with the active phase of the animals, when energy intake is usually high and available for storage. The peak in uptake of ^{3}H-activity for heart (**Figure 1D**) and muscle (**Figure 1E**) was found at ZT4, corresponding to the period of low energy intake and a required shift towards fat oxidation. For the BAT depots the [^{3}H]oleate uptake peaked just before onset of the active dark phase at ZT12, and was 17±4 % dose/g for iBAT (**Figure 1F**) and 28±19 % dose/g sBAT (**Figure 1G**), respectively. The uptake at this peak was 1.7-15 fold higher than the maximum uptake by other organs, indicating that BAT is highly metabolically active. Additionally, the difference between the minimum and maximum [^{3}H]oleate uptake by iBAT (4.3-fold) and sBAT (12.0-fold) was higher than the difference observed in liver (1.7-fold), sWAT (2.0-fold), gWAT (3.3-fold), heart (1.9-fold) and muscle (2.3-fold). The maximum uptake of [^{3}H]oleate by PVAT was 15.3-fold higher than its minimum and, therefore, comparable to other BAT depots, albeit that the peak in uptake (i.e. ZT18) was similar to WAT depots (**Figure 1H**). Most likely this discrepancy is explained by the fact that PVAT is a composed of a mixture of brown and white adipocytes.

Circadian rhythm of TG-derived fatty acid uptake adapts to photoperiod, only in BAT

Next, we assessed the ability of the various tissues to adapt the circadian rhythm of [^{3}H]oleate uptake to either a short (8h) or long (16h) photoperiod. Interestingly, the photoperiod changed the circadian [^{3}H]oleate uptake pattern only by brown adipocyte depots. Light exposure (LE) duration significantly determined [^{3}H]oleate uptake by iBAT (p-value for LE, p_{LE}=0.0034; **Figure 1F**), sBAT (p_{LE} =0.0085; **Figure 1G**) and PVAT (p_{LE} = 0.014; **Figure 1H**), but not by liver (p_{LE} = 0.141; **Figure 1A**), sWAT (p_{LE} = 0.75; **Figure 1B**), gWAT (p_{LE} = 0.3040; **Figure 1C**), heart (p_{LE} = 0.1765; **Figure 1D**) and muscle

(p_{LE} = 0.3232; **Figure 1E**). Short photoperiod increased the amplitude (*i.e.* difference between maximum and minimum uptake) of [^{3}H]oleate uptake by iBAT (264%) and sBAT (226%) compared to a photoperiod of 12h. Notably, photoperiod did not only determine amplitude, but also the timing of the maximum [^{3}H]oleate uptake by BAT. Long photoperiod delayed maximum [^{3}H]oleate uptake by iBAT from ZT12 to ZT18. Likewise, short photoperiod advanced and increased the maximum [^{3}H]oleate uptake by both iBAT and sBAT depots from ZT12 to ZT8. Strikingly, short photoperiod resulted in an increased area under the curve for [^{3}H]oleate uptake (**Figure 2A**) and increased the average [^{3}H]oleate uptake of all time points by iBAT (+190%; $p<0.05$), sBAT (+207%; $p<0.05$) and pVAT (+230%; $p<0.05$) compared to long photoperiod (**Figure 2B**). The light exposure period (h) negatively correlated with [^{3}H]oleate uptake by iBAT (R^2 = 0.107, p=0.006; **Figure 2C**), sBAT (R^2 = 0.099, p=0.010; **Figure 2D**) and PVAT (R^2 = 0.096, p=0.011; **Figure 2E**) and not by other metabolic organs (not shown).

Because changes in photoperiod specifically affected the circadian pattern of fatty acid uptake by the various brown adipocyte depots, we further investigated on the effect of photoperiod on BAT function. Since BAT activation decreases the lipid content of BAT (10) whereas BAT inactivation increases its lipid content (11), we histologically determined the daily rhythm of lipid content in BAT, and the effect of photoperiod thereon. A short photoperiod resulted in a maximum intracellular lipid depletion at time point ZT8 (**Figure 2F**) corresponding with the period of maximum uptake of [^{3}H]oleate by iBAT (**Figure 1F**). A long photoperiod delayed maximum lipid depletion to ZT18 (**Figure 2F**) at which a maximum uptake of [^{3}H]oleate by iBAT was observed (**Figure 1F**). Previously, we proposed that the SCN regulates BAT activity via the sympathetic nervous system (7). Since tyrosine hydroxylase (TH) is the rate-limiting enzyme in norepinephrine production and, therefore, a measure of sympathetic activity we next quantified TH content in BAT. The dip in lipid content at ZT8 during short photoperiod coincided with a peak in TH content in BAT (**Figure 2G**). Long photoperiod shifted the peak in TH to ZT18, corresponding to the maximum lipid depletion of BAT (**Figure 2F**) and maximum uptake of [^{3}H]oleate by iBAT (**Figure 1F**). These data indicate that the daily and seasonal rhythms in BAT activity indeed may depend on sympathetic outflow.

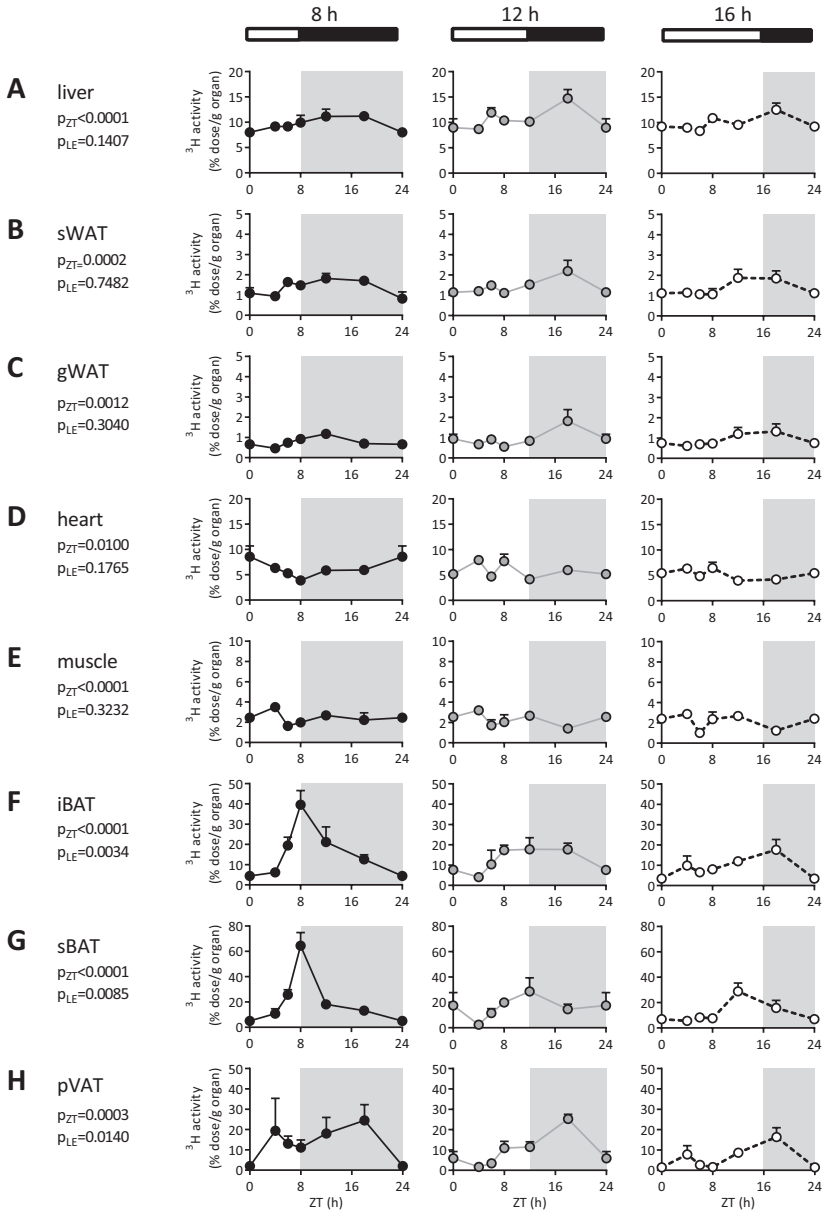

Figure 1 – Daily and seasonal rhythms in TG-derived fatty acid uptake in wild-type mice. Wild-type mice were exposed to photoperiods of 8, 12 or 16h of light per day for five weeks and injected with glycerol tri[^{3}H]oleate-labeled lipoprotein-like particles at six time points (n=3-4/group). Mice were sacrificed and uptake of [^{3}H]oleate was determined for liver (**A**), sWAT (**B**), gWAT (**C**), heart (**D**), muscle (**E**), iBAT (**F**), sBAT (**G**) and PVAT (**H**). Data are presented as means ±SEM and ZT0/ZT24 was double plotted for visualization purposes. P_{ZT} and P_{LE} represent p-values for the factors Zeitgeber Time (*i.e.* time point) and light exposure, respectively (two-way ANOVA). Abbreviations: iBAT, interscapular BAT; sBAT, subscapular BAT; pVAT, perivascular adipose tissue; sWAT, subcutaneous white adipose tissue; gWAT, gonadal white adipose tissue.

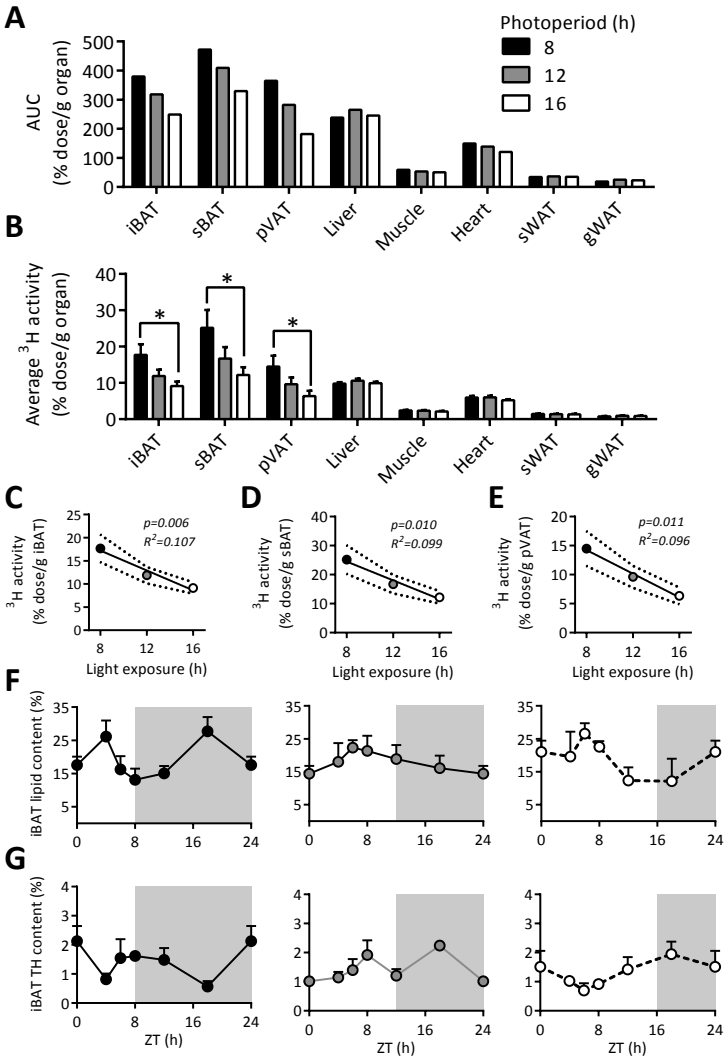

Figure 2 – Photoperiodic regulation of TG-derived fatty acid uptake by BAT of wild-type mice. Wild-type mice were exposed to photoperiods of 8, 12 or 16h of light per day for five weeks and injected with glycerol tri[^{3}H]oleate-labeled lipoprotein-like particles (n=24/group). Mice were sacrificed at six time points (ZT 0, 4, 6, 8, 12, 18) and the area under the curve (**A**) and average daily uptake of [^{3}H]oleate derived activity was determined (**B**). Interscapular BAT (iBAT) was collected for histological purposes. Intracellular lipid content was quantified from H&E stained sections (**A**) and tyrosine hydroxylase (TH) content was determined by immunohistochemistry (**B**). Data are presented as means ±SEM and ZT0/ZT24 was double plotted for visualization purposes. Correlations were made between photoperiod and uptake of [^{3}H]oleate by iBAT (**C**), sBAT (**D**) and pVAT (**E**). Interscapular BAT (iBAT) was collected for histological purposes. Intracellular lipid content was quantified from H&E stained sections (**F**) and tyrosine hydroxylase (TH) content was determined by immunohistochemistry (**G**). * $p<0.05$ (one-way ANOVA, Tukey's post-hoc test). Correlations were analyzed by linear regression. Abbreviations: iBAT, interscapular BAT; sBAT, subscapular BAT; pVAT, perivascular adipose tissue; sWAT, subcutaneous white adipose tissue; gWAT, gonadal white adipose tissue.

The daily and seasonal rhythms of BAT activity coincide with expression of thermogenic genes.

Next, we determined expression patterns of key genes involved in BAT thermogenesis (**Figure 3**). Zeitgeber Time did not significantly determine expression of *Cd36* (**Figure 3A**), lipoprotein lipase (*Lpl*; **Figure 3B**) and uncoupling protein 1 (*Ucp1*; **Figure 3C**), but did determine gene expression of deiodinase type II (*Dio2*; **Figure 3D**), *Prdm16* (**Figure 3E**), peroxisome proliferator-activated receptor gamma coactivator 1-alpha (*Pgc1a*; **Figure 3F**) and clock genes *Rev-erba* (**Figure 3G**) and period 2 (*Per2*; **Figure 3H**) in iBAT. When mice were exposed to a regular photoperiod of 12h, gene expression of *Ucp1*, *Dio2*, *Prdm16* and *Pgc1a* were highest at ZT12 and lowest at ZT18 (1.9-fold, 5.1-fold, 2.4-fold and 4.6-fold difference, respectively). Gene expression of *Rev-erba* was highest at ZT6 and lowest at ZT18 (4.6-fold difference), while expression of Per2 was highest at ZT12 and lowest at ZT4 (5.7-fold difference).

Light exposure duration significantly determined expression of *Per2* (p_{LE}=0.0126), as both long and short photoperiod shifted the rhythmic pattern. Long photoperiod only shifted the peak of *Pgc1a* expression from ZT8 to ZT12, and that of the clock genes *Rev-erba* from ZT6 to ZT8 and *Per2* from ZT12 to ZT18, while the maximum gene expression of the other genes remained at ZT12. Interestingly, short photoperiod resulted in a phase advance of the peaks in gene expression to ZT8 for *Lpl*, *Dio2* and *Prdm16*, and to ZT6 for *Ucp1* and *Pgc1a,* indicating adaptation the circadian expression of all these genes to the photoperiod.

► **Figure 3 – Daily and seasonal rhythms in gene expression in BAT of wild-type mice.** Wild-type mice were exposed to photoperiods of 8, 12 or 16h of light per day for five weeks and sacrificed at six time points (n=4/group). Interscapular BAT (iBAT) was collected for gene expression analysis. Normalized gene expression was calculated for *Cd36* (**A**), *Lpl* (**B**), *Ucp1* (**C**), *Dio2* (**D**), *Prdm16* (**E**), *Pgc1a* (**F**) and clock genes *Rev-erba* (**G**) and *Per2* (**H**). Data are presented as means ±SEM and ZT0/ZT24 was double plotted for visualization purposes.

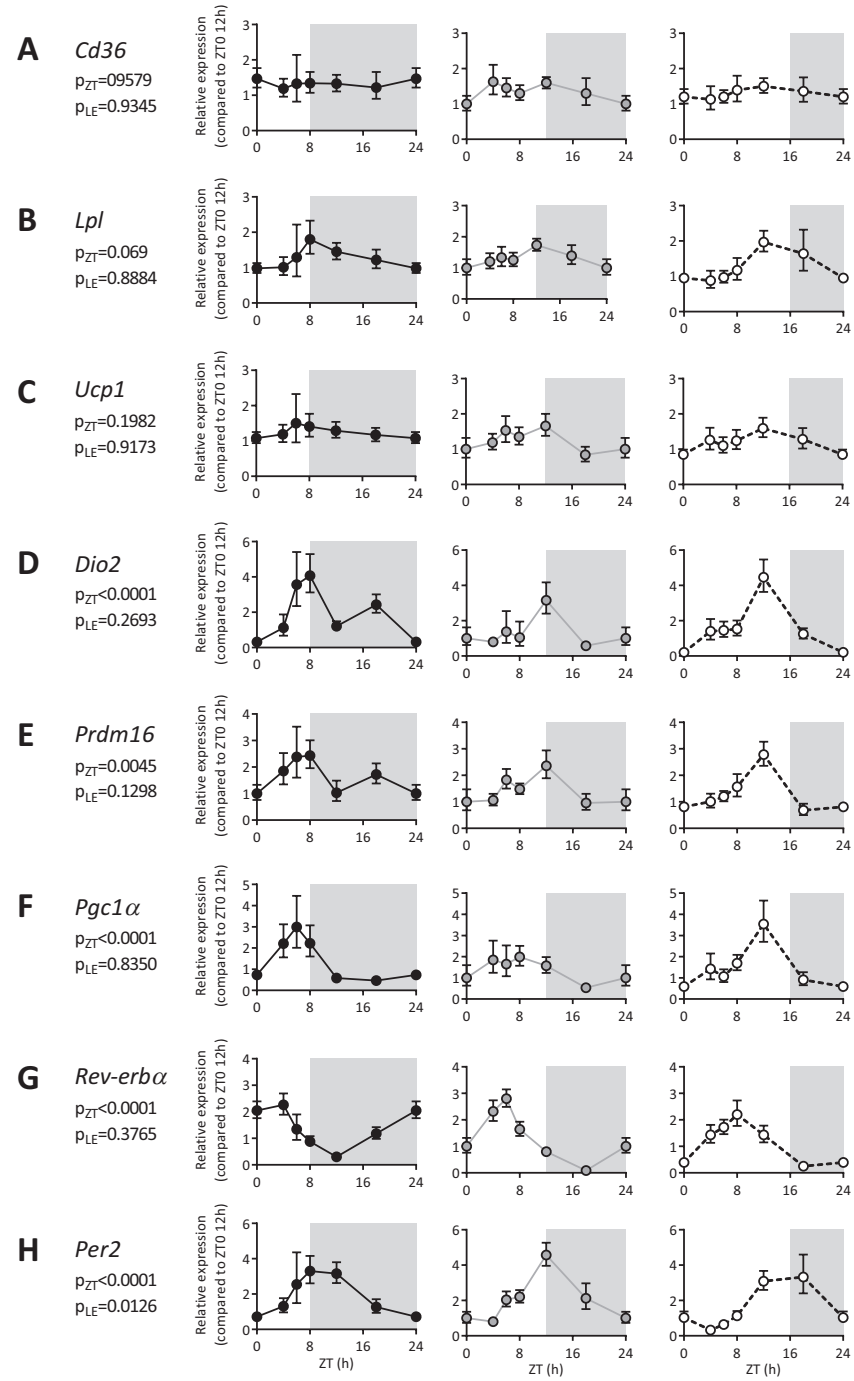
A
Cd36
pZT=09579
pLE=0.9345
B
Lpl
pZT=0.069
pLE=0.8884
C
Ucp1
pZT=0.1982
pLE=0.9173
D
Dio2
pZT<0.0001
pLE=0.2693
E
Prdm16
pZT=0.0045
pLE=0.1298
F
Pgc1α
pZT<0.0001
pLE=0.8350
G
Rev-erbα
pZT<0.0001
pLE=0.3765
H
Per2
pZT<0.0001
pLE=0.0126
Relative expression (compared to ZT0 12h)
ZT (h)

Circadian rhythm in BAT activity determines diurnal variation in plasma TG levels

Since activation of BAT importantly contributes to lowering of plasma TG levels in hyperlipidemic mice (12), we next investigated the consequences of the circadian rhythm in BAT activity on plasma TG levels in hyperlipidemic *APOE*3-Leiden.CETP* mice. Mice were exposed to a photoperiod of 10h and after 5 weeks we determined the uptake of TG-derived fatty acids by BAT and other metabolic organs at the onset of light- and dark phase. The uptake of glycerol tri[^{3}H]oleate-derived [^{3}H]oleate was higher at ZT10 compared to ZT0 for iBAT (4.2-fold; $p<0.01$), sBAT (3.8-fold; $p<0.05$) and sWAT (2.2-fold; $p<0.01$), and lower for heart (1.6-fold; $p<0.01$) (**Figure 4A**). The increase in [^{3}H]oleate uptake at ZT10 compared to ZT0 by iBAT (up to 34±6 % of injected dose/g organ) and sBAT (up to 33±10 % of injected dose/g organ) resulted in an enhanced clearance of the radiolabel from the circulation (**Figure 4B**) reflected by a 1.6-fold shorter half-life (2.8±0.2 min *vs* 4.5±1.0 min; $p<0.01$; **Figure 4C**), and was accompanied by lower plasma TG levels (7.2±1.6 mM *vs* 3.0±0.6 mM; $p<0.05$; **Figure 4D**). These data indicate that the endogenous high activity of BAT at the start of the dark phase leads to increased TG clearance and lowering of plasma TG in hyperlipidemic mice.

Discussion

In the present study we investigated daily and seasonal rhythms in BAT. We show that circadian timing as well as photoperiodic seasonal information are important for BAT activity, as demonstrated by studies evaluating TG-derived fatty acid uptake from plasma, lipid content and expression of thermogenic genes. We found that BAT activity is the highest at the onset of the active, dark period. Strikingly, short photoperiod advanced the peak in BAT activity and resulted in an increased total capacity to take up circulating lipids, while long photoperiod reduced the uptake of fatty acids by BAT. Metabolic organs other than BAT, including liver, WAT, muscle and heart, also displayed a circadian pattern in their metabolic activity but did not adapt to photoperiodic changes.

While the daily peaks in TG-derived fatty acid uptake by WAT and liver corresponded with periods of excessive energy availability (*i.e.* active period at dark phase) and the uptake by heart and muscle with the period of low carbohydrates (*i.e.* inactive period during light phase), the uptake of BAT depots reached it maximum at the onset of the dark phase. In addition, we observed high TH content, lipid depletion and high expression of key thermogenic genes at the same time, overall indicating increased BAT activity just before wakening. These patterns are in line with a previous report on circadian rhythm in glucose uptake by BAT using [^{18}F]FDG-PET-CT scanning (6) and correspond with the known rhythm in core temperature for mice, which declines

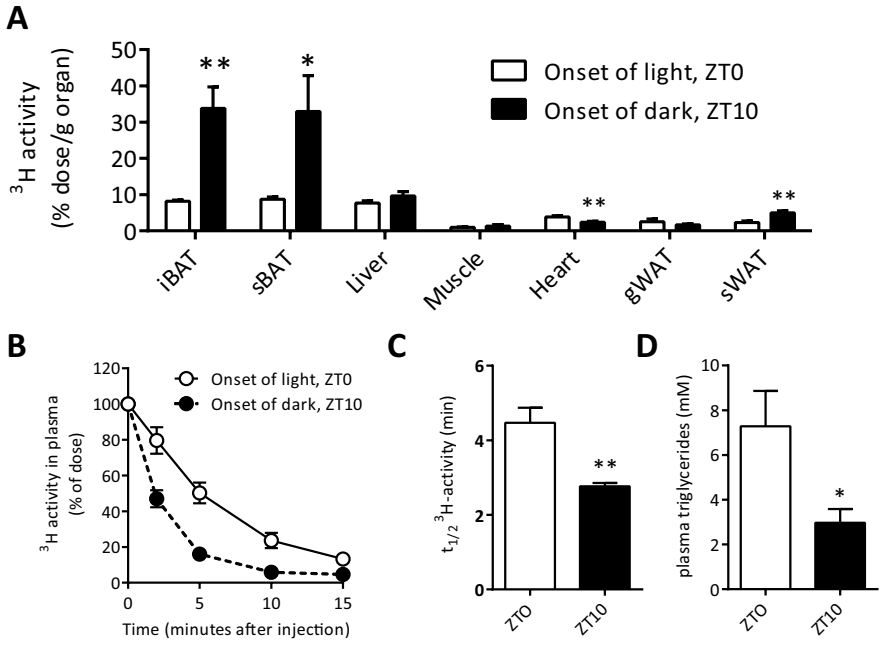

Figure 4 – Daily rhythms in TG metabolism in hyperlipidemic *APOE*3-Leiden.CETP* mice. *APOE*3-Leiden.CETP* mice were exposed to a photoperiod of 10h of light per day. After 5 weeks, mice were injected with glycerol tri[^{3}H]oleate-labeled lipoprotein-like particles at ZT0 and ZT10 (n=6/ time point). Uptake of [^{3}H]oleate by various metabolic organs was determined (**A**). [^{3}H]oleate was quantified in plasma at several time points after injection and expressed as percentage of the injected dose (**B**), and the plasma half-life of [^{3H}]oleate was calculated (**C**). Triglycerides were measured in plasma at the onset and light phase (ZT0) and dark phase (ZT10) (**D**). Data are presented as means ±SEM. *p<0.05, **p<0.01 (T-test). Abbreviations: iBAT, interscapular BAT; sBAT, subscapular BAT; pVAT, perivascular adipose tissue; sWAT, subcutaneous white adipose tissue; gWAT, gonadal white adipose tissue.

during sleep and rises before wake (13). The pronounced gene in *Pgc1a*, *Ucp1*, *Prdm16* and *Dio2* are in line with previous reports of gene expression under normal photoperiod regimes (3,14,15). The rhythmicity of *Ucp1* seems less consistent as one study found a high amplitude (3) while others reported weaker rhythmicity (15) similar to the present data. A possible explanation for this discordance is that *Ucp1* expression may be more influenced by fasting or feeding of the mice, since the feeding state varies across the different studies.

We found large differences in uptake of TG-derived fatty acids and expression of genes involved in thermogenesis, including *Prdm16* and *Pgc1a*, by BAT along the day, indicating that disturbed circadian rhythmicity may have considerable effects on BAT function and adiposity. Indeed, genetic mouse models of circadian dysfunction,

among others *Clock*$^{mt/mt}$ mice (16) and *Per2*$^{-/-}$ mice (17), are prone to develop obesity. In addition lesioning of the SCN and continuous light exposure result in disturbed circadian behavior and acute weight gain (7,18,19). However, these severe models for disturbed circadian rhythmicity can be considered as a pathophysiological condition. In the current study, exposure to a photoperiod of 16h was sufficient to severely diminish the uptake of TG-derived fatty acids by BAT when compared to short photoperiod, which most likely corresponded with lower energy expenditure. Comparable, hibernating animals typically increase their food intake and decrease energy expenditure during summer, resulting in lipid deposition in WAT (20). Conversely, during winter hibernating animals almost exclusively rely on lipid oxidation. These changes in energy expenditure can partly be mimicked by exposing animals to different photoperiods under laboratory conditions (20). Interestingly, this regulation of energy balance by photoperiod is not limited to hibernating animals. Switching photoperiod in field voles to a length of 16h increases body weight by 24% in 4 weeks compared to animals that remained on a photoperiod of 8h (21). Further, it has been reported that overweight and obese children experience accelerated weight gain during the summer (22), suggesting that photoperiodic regulation of energy expenditure may apply to humans as well.

It is tempting to speculate why especially BAT is sensitive to changes in photoperiod, reflecting seasonal regulation, with respect to TG uptake, compared to other metabolic organs such as white adipose tissue, liver, muscle and heart. Heat production by BAT is activated whenever the animal is in need of extra heat, *e.g.* during arousal from hibernation or upon wakening, so a possible explanation is the adaptation to photoperiodic changes in sleep-wake pattern (23). However, this does probably not explain the change in overall daily capacity of BAT to take up TG-derived fatty acids as observed within our study. As noted before, detectability of human BAT by [^{18F}]FDG PET-CET scans at room temperature displays a stronger correlation with photoperiod than ambient temperature (6), and changes in photoperiod and BAT detectability seem to occur before changes in outside temperature. Therefore, a change in photoperiod likely signals to BAT to be prepared for upcoming seasonal changes, as in general, changes in photoperiod precede changes in ambient temperature.

Despite the increasing interest in circadian clock research, the exact mechanism how light information is perceived by the eye and transmitted to the periphery is not fully understood. Lesioning of the SCN does not lead to loss of cyclic activity in metabolic organs, but does prevent synchronization of peripheral clocks to the environment (24). As synchronization of peripheral clocks occurs during seasonal adaptation, the SCN is likely crucial for the regulation of seasonal adaptation. Studies reported that the SCN communicates to the periphery via the autonomic nervous system, via hormonal cues such as corticosterone and melatonin, and via rhythmic

behavior (25). Considering the importance of the sympathetic activity for cold-induced thermogenesis (1,26) and the direct neuronal connection between the SCN and BAT (1), it is likely that the autonomic nervous system regulates circadian and seasonal rhythmicity in BAT. Compatible with this hypothesis, in this study we found peaks in TH content of BAT occurring simultaneously with lipid depletion in BAT, uptake of TG-derived fatty acids by BAT and expression of thermogenic genes in BAT. In addition, we recently demonstrated that prolonged daily light exposure diminishes BAT activity, an effect that was abolished by surgical sympathetic denervation of the tissue (7).

In summary, we identified circadian and seasonal rhythms in BAT activity, contributing to diurnal rhythmicity in TG plasma levels in dyslipidemic mice. Future studies should reveal to what extent these data can be extrapolated to humans. At least in light of pre-clinical research on BAT activity, but potentially also in clinical research, timing of experiments clearly is a crucial factor that should be carefully considered.

Acknowledgements

This work was supported by the Netherlands Organization for Scientific Research (NWO-VENI grant 016.136.125 to NR Biermasz), the European Foundation for the Study of Diabetes and the Programme Partner Novo Nordisk (grant 94802 to CP Coomans, JH Meijer and PCN Rensen) and the Dutch Diabetes Research Foundation (grant 2013.81.1663 to CP Coomans). PCN Rensen is an Established Investigator of the Netherlands Heart Foundation (grant 2009T038). The authors declare no conflict of interest.

References

1. Bamshad, M., Song, C. K., & Bartness, T. J. (1999) CNS origins of the sympathetic nervous system outflow to brown adipose tissue. *Am J Physiol* 276, R1569-R1578.
2. Amir, S., Shizgal, P., & Rompre, P. P. (1989) Glutamate injection into the suprachiasmatic nucleus stimulates brown fat thermogenesis in the rat. *Brain Res* 498, 140-144.
3. Yang, X., Downes, M., Yu, R. T. *et al.* (2006) Nuclear receptor expression links the circadian clock to metabolism. *Cell* 126, 801-810.
4. Gerhart-Hines, Z., Feng, D., Emmett, M. J. *et al.* (2013) The nuclear receptor Rev-erbalpha controls circadian thermogenic plasticity. *Nature* 503, 410-413.
5. VanderLeest, H. T., Houben, T., Michel, S. *et al.* (2007) Seasonal encoding by the circadian pacemaker of the SCN. *Curr Biol* 17, 468-473.
6. van der Veen, D. R., Shao, J., Chapman, S. *et al.* (2012) A diurnal rhythm in glucose uptake in brown adipose tissue revealed by in vivo PET-FDG imaging. *Obesity (Silver Spring)* 20, 1527-1529.
7. Kooijman, S., van den Berg, R., Ramkisoensing, A. *et al.* (2015) Prolonged daily light exposure increases body fat mass through attenuation of brown adipose tissue activity. *Proc Natl Acad Sci USA*.
8. Westerterp, M., van der Hoogt, C. C., de, H. W. *et al.* (2006) Cholesteryl ester transfer protein decreases high-density lipoprotein and severely aggravates atherosclerosis in APOE*3-Leiden mice. *Arterioscler Thromb Vasc Biol* 26, 2552-2559.
9. Rensen, P. C., Herijgers, N., Netscher, M. H. *et al.* (1997) Particle size determines the specificity of apolipoprotein E-containing triglyceride-rich emulsions for the LDL receptor versus hepatic remnant receptor in vivo. *J Lipid Res* 38, 1070-1084.
10. Berbee, J. F., Boon, M. R., Khedoe, P. P. *et al.* (2015) Brown fat activation reduces hypercholesterolaemia and protects from atherosclerosis development. *Nat Commun* 6, 6356.
11. Kooijman, S., Boon, M. R., Parlevliet, E. T. *et al.* (2014) Inhibition of the central melanocortin system decreases brown adipose tissue activity. *J Lipid Res* 55, 2022-2032.
12. Bartelt, A., Bruns, O. T., Reimer, R. *et al.* (2011) Brown adipose tissue activity controls triglyceride clearance. *Nat Med* 17, 200-205.
13. Refinetti, R. (2012) Integration of biological clocks and rhythms. *Compr Physiol* 2, 1213-1239.
14. Hatori, M., Vollmers, C., Zarrinpar, A. *et al.* (2012) Time-restricted feeding without reducing caloric intake prevents metabolic diseases in mice fed a high-fat diet. *Cell Metab* 15, 848-860.
15. Paschos, G. K., Ibrahim, S., Song, W. L. *et al.* (2012) Obesity in mice with adipocyte-specific deletion of clock component Arntl. *Nat Med* 18, 1768-1777.
16. Turek, F. W., Joshu, C., Kohsaka, A. *et al.* (2005) Obesity and metabolic syndrome in circadian Clock mutant mice. *Science* 308, 1043-1045.
17. Yang, S., Liu, A., Weidenhammer, A. *et al.* (2009) The role of mPer2 clock gene in glucocorticoid and feeding rhythms. *Endocrinology* 150, 2153-2160.
18. Coomans, C. P., van den Berg, S. A., Houben, T. *et al.* (2013) Detrimental effects of constant light exposure and high-fat diet on circadian energy metabolism and insulin sensitivity. *FASEB J* 27, 1721-1732.
19. Coomans, C. P., van den Berg, S. A., Lucassen, E. A. *et al.* (2013) The suprachiasmatic nucleus controls circadian energy metabolism and hepatic insulin sensitivity. *Diabetes* 62, 1102-1108.
20. Dark, J. (2005) Annual lipid cycles in hibernators: integration of physiology and behavior. *Annu Rev Nutr* 25, 469-497.
21. Krol, E., Redman, P., Thomson, P. J. *et al.* (2005) Effect of photoperiod on body mass, food intake and body composition in the field vole, Microtus agrestis. *J Exp Biol* 208, 571-584.
22. Baranowski, T., O'Connor, T., Johnston, C. *et al.* (2014) School year versus summer differences in child

weight gain: a narrative review. *Child Obes* 10, 18-24.
23. Deboer, T. & Tobler, I. (1996) Shortening of the photoperiod affects sleep distribution, EEG and cortical temperature in the Djungarian hamster. *J Comp Physiol A* 179, 483-492.
24. Cailotto, C., La Fleur, S. E., Van, H. C. *et al.* (2005) The suprachiasmatic nucleus controls the daily variation of plasma glucose via the autonomic output to the liver: are the clock genes involved? *Eur J Neurosci* 22, 2531-2540.
25. Buijs, R. M. & Kalsbeek, A. (2001) Hypothalamic integration of central and peripheral clocks. *Nat Rev Neurosci* 2, 521-526.
26. Tupone, D., Madden, C. J., & Morrison, S. F. (2014) Autonomic regulation of brown adipose tissue thermogenesis in health and disease: potential clinical applications for altering BAT thermogenesis. *Front Neurosci* 8, 14.